

Growth and Characterization of Al₂O₃ Ultra-Thin Film as a Passivation Layer for Silicon Solar Cells

Mateus Manuel Neto^{1,3}, Luu Thi Lan Anh^{1*}, Nguyen Trung Do¹, Nguyen Hoang Thoan¹,
Nguyen Ngoc Trung¹, Chung Han Wu², Vo Thach Son¹

¹ Hanoi University of Science and Technology, No. 1, Dai Co Viet, Hai Ba Trung, Hanoi, Viet Nam

² Boviet Solar Technology Co.LTD

³ Agostinho Neto University, Avenida 4 de Fevereiro 7 Luanda, Angola

Received: January 17, 2018; Accepted: June 25, 2018

Abstract

The properties of aluminum oxide (Al₂O₃) films have shown excellent performances such as remarkable passivation behaviors on both n- and p-type Si surfaces. For fabrication of Al₂O₃ one can use a cost-saving deposition technique called atomic layer deposition (ALD). This study explores the conditions necessary for low temperature fabrication of Al₂O₃ thin films by the ALD technique. Properties of the Al₂O₃ thin films were analysed by variable-angle spectroscopic ellipsometer (VASE) and X-ray photoemission spectroscopy (XPS). Thicknesses of the films were investigated depending on deposition cycles. The estimated deposition growth rate was 1.0 Å/cycle at deposition temperature of about 200°C. The Al₂O₃ ultra-thin films can be used as a passivation layer for Si thin film solar cells.

Keywords: atomic layer deposition ALD, Al₂O₃ ultra-thin film, interface passivation, Si solar cells

1. Introduction

An excellent interface passivation has been considered as a key point for high efficiency solar cells as passivated emitter and rear cell. To suppress the surface/interface recombination, two fundamental methods are applied: (i) the reduction of interface trap density D_{it} (known as chemical passivation); (ii) the reduction of electrons or holes concentration at the surface (defined as field-effect passivation), which are so-called surface passivation techniques [1,2,3].

The properties of aluminum oxide (Al₂O₃) films have been widely investigated for solar cell fabrication. The films have shown excellent performances such as remarkable passivation behavior on both n- and p-type Si surfaces and the cost-saving deposition using atomic layer deposition (ALD) at low temperatures [2-8].

Recently, for growing high quality thin films, ALD technique is more preferred than conventional methods, because it provides precise, uniform, low temperature and self-terminating layers of desired material. The self-termination property can be defined as the ability of reactants to stop automatically when they all react with the prepared sites. This property allows to deposit almost one monolayer in each half cycle even if the dosage time

is more than what is required. Each ALD deposition consists of the following steps: (i) deposition of the first reactant, (ii) purge of the nonreacted reactants and volatile products from the first step with inert gas, (iii) deposition of the second reactant and (iv) purge of the non-reacted reactants and volatile products from the third step.

This study explores the conditions necessary for low temperature deposition of Al₂O₃ thin films by the ALD technique and examines properties of the resulting films.

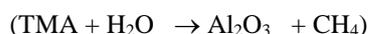
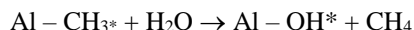
2. Experimental

TMA (Al(CH₃)₃) and water were used as the metal and oxygen precursors. The films were deposited in a SYSKEY ALD system. (100)-oriented Si wafers with the diameter of 15 cm were used as the substrates. Before experiments, the wafers were cleaned using RCA method and followed by a diluted HF dip to remove the Si native oxide layer. The TMA precursor and H₂O precursor were holden at 18°C. The films were grown at a temperature in a range of 200-300°C. Nitrogen (N₂) gas was used as a carrier gas with pressure of about 2.4×10⁻¹ Torr.

A cycle of the reaction consisted of a 20 ms injection of TMA vapor followed by 8 s N₂ purge and a 20 ms injection of H₂O vapor followed by 8 s N₂ purge. The deposition rate is estimated to be around 0.125 nm/cycle. ALD process is based on sequential, self-limiting surface chemical "half-reactions".

* Corresponding author: Tel.: (+84) 989659488
Email: anh.luuthilan@hust.edu.vn

The TMA and H₂O yield Al₂O₃ ALD according to the following two reactions:



where the asterisk designates the surface species. The main driving force for the efficient reactions is the formation of a very strong Al–O bond. Therefore, Al₂O₃ film thickness could be controlled accurately by controlling the number of reaction cycles. It should be noted here that there are some residual Al–OH* bonds during the reaction. O–H bonds would be easily broken, resulting in the interstitial H atoms within the Al₂O₃ matrix. The numbers of deposition cycles were 50, 100, 150 and 200.

Thicknesses and refractive indices of the obtained Al₂O₃ thin films were measured using a SE800 variable-angle spectroscopic ellipsometer (VASE). Measurements were obtained over the spectral range from 280 to 1700 nm using the incident angles of 64, 69 and 75°. VASE is routinely used in optical characterization and film thickness determination. The ellipsometric method of optically measuring the thickness of thin nonabsorbing films on absorbing substrates is well known and hence will not be discussed in detail here. In principle, if plane polarized light is incident on a clean absorbing substrate at an arbitrary angle, the reflected light will be elliptically polarized. The ellipticity parameters, amplitude ratio Psi ψ and phase shift delta Δ between reflected p- and s-polarized beams, of the reflected light are considerably different if a thin non absorbing film is present on the surface, thus providing a means of measuring the thickness of the thin film with high precision, provided its refractive index is known. The ellipsometric spectra can be fitted to the optical model based on the film structure, then the optical

properties and film thickness of the measured material can be revealed. Its noncontact, nondestructive characteristics are ideal for many situations when film thickness or dielectric constants are needed [11].

X-ray photoemission spectroscopy (XPS) studies were generally performed on a Quanter SXM spectrometer with a high-resolution X-ray monochromator, using an Al K α at 1486.6 eV. General calibration produced a binding energy scale specified with X-ray beam by $I_e = 2.6$ mA. Power is about 50 W and beam size is about 200 μm (mappings are often done with beam sizes down to 9 μm). Auto-Z height : 23.95 mm and up, depending on platen position, done with the 5 μm 1.25W15keV X-ray beam at the standard beam-input and detector input angle of 45°. Auto-Z is necessary for alignment of the surface of the sample with the foci of X-ray source and electron analyzer. Fitting of spectra (using Multipak v.9.6.0.15 software) is mostly done after shifting of the measured spectra with respect to known reference binding energies. Aliphatic carbon C_{1s} at 284.8 eV or gold Au_{4f7/2} at 83.96 eV, silver Ag_{3d5/2} at 368.21 eV and copper Cu_{2p3/2} at 932.62 eV.

3. Results and discussion

Figures 1 illustrates the measured values of the ellipsometric parameters Psi and Delta for the sample deposited at 200 cycles, respectively, with different incident angles. In this study, the optical fitting models include a Si substrate, a SiO₂ native oxide layer (~1.5 nm) and an Al₂O₃ layer. From fitting results, the thickness of the 200-cycle film was estimated of 19.95 \pm 0.01 nm. VASE measurements and fitting were also done for other samples deposited at 50, 100 and 150 cycles, resulting thicknesses of 4.94 \pm 0.01, 10.03 \pm 0.01, 15.16 \pm 0.01, respectively.

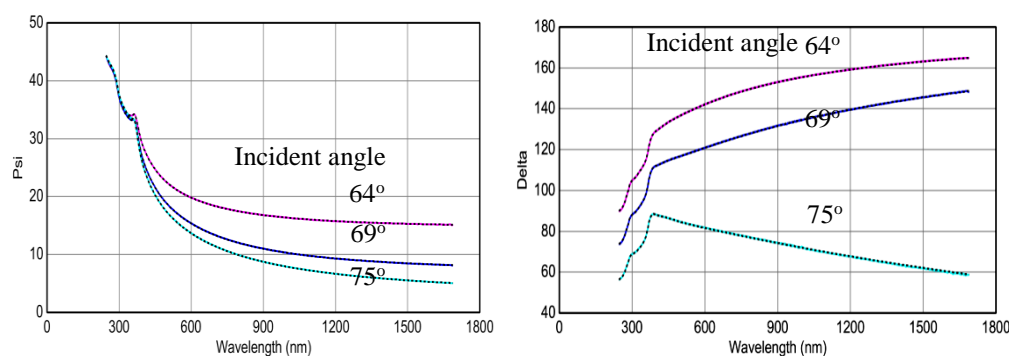


Fig. 1. Spectroscopic ellipsometry measurements for the sample deposited at 200 cycles: (left) amplitude ratio Psi (in percentage) with WVASE32 parameter fitting, and (right) phase shift delta (in degree) with WVASE32 parameter fitting. The measurements were carried out with different incident angles.

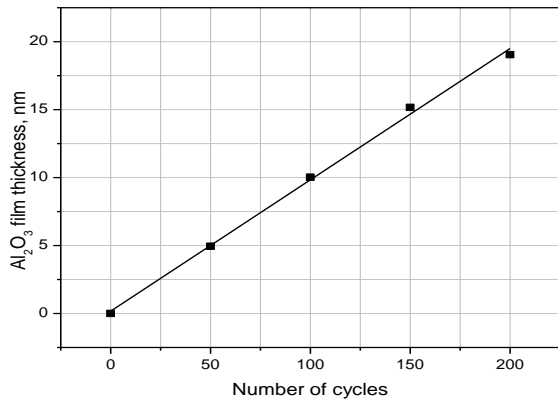


Fig. 2. Al₂O₃ film thickness as a function of the number of ALD cycles ($T_{\text{dep}} \approx 200^\circ\text{C}$).

Figure 2 illustrates the Al₂O₃ film thickness dependence on ALD cycles as revealed by VASE fitting. It can be found that with increasing deposition cycles, the thickness of Al₂O₃ film increases. From figure 2, we can know that the Al₂O₃ films were grown at a speed of 1.0 Å/cycle. The growth rate becomes stable when ALD cycle is higher than 50.

Because Al₂O₃ is a transparent invisible region, the optical model of Al₂O₃ used in ellipsometry fitting is Cauchy model, which is defined as follows:

$$n(\lambda) = A + \frac{B}{\lambda^2} + \frac{C}{\lambda^4} \quad (1)$$

where A, B, and C are the material coefficients that define the real part of the refractive index $n(\lambda)$.

Figure 3 shows the refractive index n and extinction coefficient k as functions of wavelength for the sample deposited at 200 cycles. We found that the refractive index n varies in a relatively narrow range about the wavelength of 550 nm.

XPS measurement in the binding energy range of 51345 eV was used to investigate the chemical composition and binding states of the Al₂O₃ films. The recorded binding energy profiles are shown in figure 4. The survey spectrum shows the peaks corresponding to the binding energies of Al, O and C. The presence of the C1s peak is advantageous as contaminant carbon can compensate the surface charging effect. The peaks observed at binding energies of 74.1 ± 0.2 eV and 531.4 ± 0.2 eV can be attributed to Al2p and O1s, respectively. These binding energies are in good agreement with the binding energies of Al₂O₃ films reported in literature [8,9,10]. Element high resolution spectra scans were made with a better energy resolution and lower noise than the survey spectrum (as shown in figure 5). From high XPS spectra, the atomic concentrations of the elements measured can be calculated and chemical shifts will show up for certain compound materials.

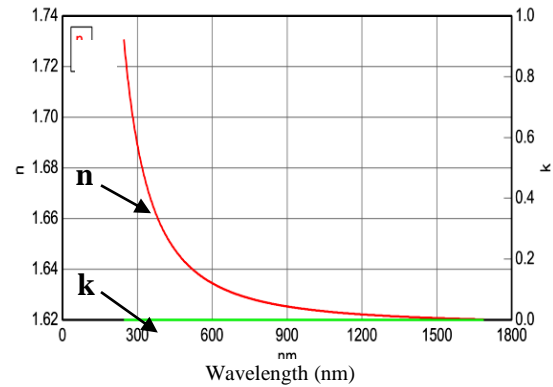


Fig. 3. Refractive index (n) and extinction coefficient (k) as functions of wavelength of the 200-cycle Al₂O₃ sample.

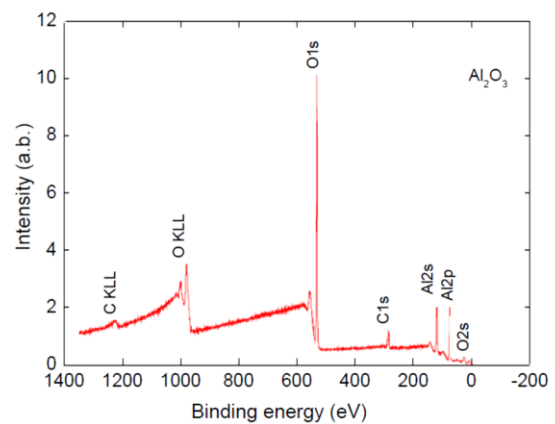


Fig. 4. XPS survey spectrum of Al₂O₃ film deposited at 200 cycles.

The atomic concentration is calculated by using the following equation

$$C_x = \frac{A_x/S_x}{\sum_i A_i/S_i} \quad (2)$$

with A_i the peak area off a photoelectron peak and S_i the relative sensitivity factor of the peak ($S_{\text{O}}=0.711$, and $S_{\text{Al}}=0.234$). The atomic concentration and O/Al atomic ratio of the sample deposited at 200 cycles show on Table 1. Table 1 also tabulates XPS main-peak's parameters including peak position and their full width at half maximum (FWHM).

Table 1. XPS main-peak parameters, atomic concentration, and O/Al atomic ratio of the 200-cycle sample.

	O-1s	Al-2p	O/Al ratio
Peak position	531.4 eV	74.1 eV	
FWHM	3.01 eV	2.72 eV	
Atomic concentration	60.17 %	27.22 %	2.21

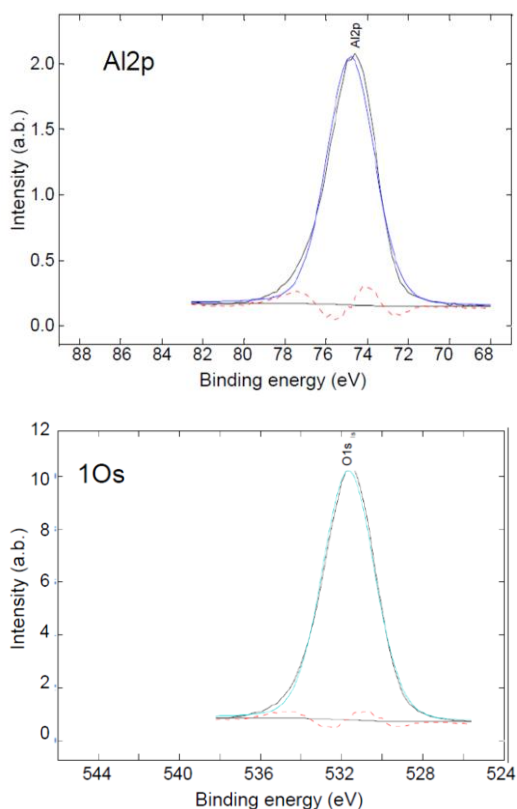


Fig. 5. High resolution XPS spectra of Al2p and O1s for Al₂O₃ film deposited at 200 cycles.

It can be found that the Al2p peak could be fitted with only one peak, suggesting that aluminum may be present only in the form of Al₂O₃ in the films. The Al2p binding energy of 74.1 ± 0.2 eV is within the range of values reported in references [8,9,10]. The major peak at the binding energy of 531.3 eV can be assigned to oxygen bonded to aluminum in Al₂O₃.

The difference between the binding energy values of O1s (bonded) and Al2p is 457.2 ± 0.4 eV, which is consistent with the O-Al-O bonding in Al₂O₃ reported by Khatibani et al. [8].

4. Conclusion

The Al₂O₃ ultra-thin films have been grown by ALD technique. The film thicknesses were investigated depending on deposition cycles. The associated growth rate was 1.0 Å/cycle at deposition temperature of about 200°C. The O1s binding energy is 531.4 ± 0.2 eV and the Al2p binding energy is 74.1 ± 0.2 eV. The carbon content in the films deposited at the temperature of 200°C was about 12.61 at. %.

Acknowledgments

This research is funded by Vietnam National Foundation for Science and Technology Development (NAFOSTED) under grant number 103.02-2015.1. We gratefully acknowledge Tom Aarnink (Faculty of Electrical Engineering, Mathematics & Computer Science, University of Twente) for the VASE and XPS measurements.

References

- [1] J. Schmidt, A. Merkle, R. Brendel, B. Hoex, M.C.M. van de Sanden and M.C. M. Kessels, Surface Passivation of High-efficiency Silicon Solar Cells by Atomic-layer-deposited Al₂O₃, Prog. Photovolt: Res. Appl. 16 (2008) 461- 466.
- [2] R.W. Johnson, A. Hultqvist and S.F. Bent, A brief review of atomic layer deposition: from fundamentals to applications, Materials Today 17 (5) (2014) 1-11.
- [3] R. Bock, S. Mau, J. Schmidt and R. Brendel, Back junction back-contact n-type silicon solar cells with screen-printed aluminum-alloyed emitter, Appl. Phys. Lett. 96 (2010) 263507-4.
- [4] Y. Xiang, C. Zhou, E. Jia and W. Wang, Oxidation precursor dependence of atomic layer deposited Al₂O₃ films in a-Si:H(i)/Al₂O₃ surface passivation stacks, Nanoscale Research Letters 10 (2015) 137-8.
- [5] L.Q. Zhu, Y.H. Liu, H.L. Zhang, H. Xiao, L.Q. Guo, Atomic layer deposited Al₂O₃ films for anti-reflectance and surface passivation applications, Appl Surf Sci. 288 (2014) 430-334.
- [6] D.K. Simon, P.M. Jordan, I. Dimstorfer, F. Benner, C. Richter, T. Mikolajick, Symmetrical Al₂O₃ based passivation layers for p- and n-type silicon, Solar Energy Materials & Solar Cells 131 (2014) 72-76.
- [7] E.C. Onyiriuka, Aluminum, titaniumboride, and nitride films sputter-deposited from multi component alloy targets studied by XPS, Applied Spectroscopy 47(1) (1993) 35-37.
- [8] A.B. Khatibani, S. Rozati, Growth and molarity effects on properties of alumina thin films obtained by spray pyrolysis, Mat. Sci. Semicon. Proc. 18 (2014) 80-87.
- [9] B.P. Dhonge, T. Mathews, S. Sundari, C. Thinaharan, M. Kamruddin, S. Dash, A. Tyagi, Spray pyrolytic deposition of transparent aluminum oxide (Al₂O₃) films, Appl. Surf. Sci. 258 (2011) 1091-1096.
- [10] G. Gauglitz and D.S. Moore, Handbook of Spectroscopy (2014) 1523-1556.
- [11] J. Haeberle, K. Henkel, H. Gargouri, F. Naumann, B. Gruska, M. Arens, M. Tallarida and D. Schmeißer, Ellipsometry and XPS comparative studies of thermal and plasma enhanced atomic layer deposited Al₂O₃-films, Beilstein J. Nanotechnol. 4 (2013) 732-742.